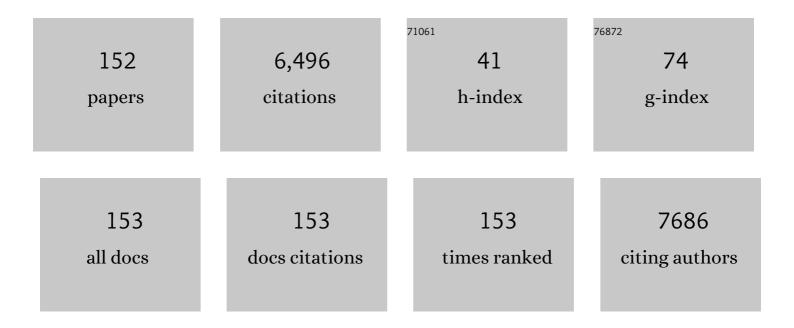
List of Publications by Year in descending order

Source: https://exaly.com/author-pdf/5717334/publications.pdf Version: 2024-02-01



#	Article	IF	CITATIONS
1	In Situ Study of FePt Nanoparticlesâ€Induced Morphology Development during Printing of Magnetic Hybrid Diblock Copolymer Films. Advanced Functional Materials, 2022, 32, 2107667.	7.8	3
2	Biopolymerâ€Templated Deposition of Ordered and Polymorph Titanium Dioxide Thin Films for Improved Surfaceâ€Enhanced Raman Scattering Sensitivity. Advanced Functional Materials, 2022, 32, 2108556.	7.8	12
3	Interpreting SAXS data recorded on cellulose rich pulps. Cellulose, 2022, 29, 117-131.	2.4	5
4	In Situ GISAXS Observation and Large Area Homogeneity Study of Slot-Die Printed PS- <i>b</i> -P4VP and PS- <i>b</i> -P4VP/FeCl <sub>3</sub> Thin Films. ACS Applied Materials & Interfaces, 2022, 14, 3143-3155.	4.0	4
5	The Influence of CsBr on Crystal Orientation and Optoelectronic Properties of MAPbl <sub>3</sub> -Based Solar Cells. ACS Applied Materials & Interfaces, 2022, 14, 2958-2967.	4.0	18
6	Hierarchical propagation of structural features in protein nanomaterials. Nanoscale, 2022, 14, 2502-2510.	2.8	6
7	Nanofibril Alignment during Assembly Revealed by an X-ray Scattering-Based Digital Twin. ACS Nano, 2022, , .	7.3	7
8	Solvent Tuning of the Active Layer Morphology of Nonâ€Fullerene Based Organic Solar Cells. Solar Rrl, 2022, 6, .	3.1	4
9	State of the art of ultra-thin gold layers: formation fundamentals and applications. Nanoscale Advances, 2022, 4, 2533-2560.	2.2	10
10	Revealing Donor–Acceptor Interaction on the Printed Active Layer Morphology and the Formation Kinetics for Nonfullerene Organic Solar Cells at Ambient Conditions. Advanced Energy Materials, 2022, 12, .	10.2	40
11	In Situ Monitoring of Scale Effects on Phase Selection and Plasmonic Shifts during the Growth of AgCu Alloy Nanostructures for Anticounterfeiting Applications. ACS Applied Nano Materials, 2022, 5, 3832-3842.	2.4	7
12	Timeâ€Resolved Orientation and Phase Analysis of Lead Halide Perovskite Film Annealing Probed by In Situ GIWAXS. Advanced Optical Materials, 2022, 10, .	3.6	22
13	Oblique angle deposited FeCo multilayered nanocolumnar structure: Magnetic anisotropy and its thermal stability in polycrystalline thin films. Applied Surface Science, 2022, 590, 153056.	3.1	6
14	Template-Induced Growth of Sputter-Deposited Gold Nanoparticles on Ordered Porous TiO <sub>2</sub> Thin Films for Surface-Enhanced Raman Scattering Sensors. ACS Applied Nano Materials, 2022, 5, 7492-7501.	2.4	11
15	Effect of Solvent Vapor Annealing on Diblock Copolymer-Templated Mesoporous Si/Ge/C Thin Films: Implications for Li-Ion Batteries. ACS Applied Nano Materials, 2022, 5, 7278-7287.	2.4	2
16	Sprayed Nanometer-Thick Hard-Magnetic Coatings with Strong Perpendicular Anisotropy for Data Storage Applications. ACS Applied Nano Materials, 2022, 5, 8741-8754.	2.4	1
17	Real-Time Observation of Temperature-Induced Surface Nanofaceting in M-Plane α-Al <sub>2</sub> O <sub>3</sub> . ACS Applied Materials & Interfaces, 2022, 14, 31373-31384.	4.0	2
18	Real-time insight into nanostructure evolution during the rapid formation of ultra-thin gold layers on polymers. Nanoscale Horizons, 2021, 6, 132-138.	4.1	24

#	Article	IF	CITATIONS
19	Insights into Growth Kinetics of Colloidal Gold Nanoparticles: In Situ SAXS and UV–Vis Evaluation. Journal of Physical Chemistry C, 2021, 125, 1087-1095.	1.5	23
20	Layer-by-Layer Spray-Coating of Cellulose Nanofibrils and Silver Nanoparticles for Hydrophilic Interfaces. ACS Applied Nano Materials, 2021, 4, 503-513.	2.4	24
21	Exploring the Effects of Different Cross-Linkers on Lignin-Based Thermoset Properties and Morphologies. ACS Sustainable Chemistry and Engineering, 2021, 9, 1692-1702.	3.2	43
22	Revealing the growth of copper on polystyrene-block-poly(ethylene oxide) diblock copolymer thin films with in situ GISAXS. Nanoscale, 2021, 13, 10555-10565.	2.8	11
23	Surface Etching of Polymeric Semiconductor Films Improves Environmental Stability of Transistors. Chemistry of Materials, 2021, 33, 2673-2682.	3.2	13
24	Tailoring the Optical Properties of Sputter-Deposited Gold Nanostructures on Nanostructured Titanium Dioxide Templates Based on In Situ Grazing-Incidence Small-Angle X-ray Scattering Determined Growth Laws. ACS Applied Materials & Interfaces, 2021, 13, 14728-14740.	4.0	4
25	Selective Silver Nanocluster Metallization on Conjugated Diblock Copolymer Templates for Sensing and Photovoltaic Applications. ACS Applied Nano Materials, 2021, 4, 4245-4255.	2.4	14
26	Humidityâ€Induced Nanoscale Restructuring in PEDOT:PSS and Cellulose Nanofibrils Reinforced Biobased Organic Electronics. Advanced Electronic Materials, 2021, 7, 2100137.	2.6	11
27	Tailoring Ordered Mesoporous Titania Films via Introducing Germanium Nanocrystals for Enhanced Electron Transfer Photoanodes for Photovoltaic Applications. Advanced Functional Materials, 2021, 31, 2102105.	7.8	9
28	Nanocellulose-Assisted Thermally Induced Growth of Silver Nanoparticles for Optical Applications. ACS Applied Materials & Interfaces, 2021, 13, 27696-27704.	4.0	10
29	Multidimensional Morphology Control for PSâ€bâ€P <sub>4</sub> VP Templated Mesoporous Iron (III) Oxide Thin Films. Advanced Materials Interfaces, 2021, 8, 2100141.	1.9	6
30	Surface characterization and resistance changes of silver-nanowire networks upon atmospheric plasma treatment. Applied Surface Science, 2021, 550, 149362.	3.1	6
31	Morphology Transformation Pathway of Block Copolymerâ€Directed Cooperative Selfâ€Assembly of ZnO Hybrid Films Monitored In Situ during Slotâ€Die Coating. Advanced Functional Materials, 2021, 31, 2105644.	7.8	11
32	Structure Development of the Interphase between Drying Cellulose Materials Revealed by In Situ Grazing-Incidence Small-Angle X-ray Scattering. Biomacromolecules, 2021, 22, 4274-4283.	2.6	8
33	Percolation of rigid fractal carbon black aggregates. Journal of Chemical Physics, 2021, 155, 124902.	1.2	17
34	Real-time observation of nucleation and growth of Au on CdSe quantum dot templates. Scientific Reports, 2021, 11, 18777.	1.6	2
35	<i>Operando</i> structure degradation study of PbS quantum dot solar cells. Energy and Environmental Science, 2021, 14, 3420-3429.	15.6	17
36	Modification of cellulose through physisorption of cationic bio-based nanolatexes – comparing emulsion polymerization and RAFT-mediated polymerization-induced self-assembly. Green Chemistry, 2021, 23, 2113-2122.	4.6	8

#	Article	IF	CITATIONS
37	Degradation mechanisms of perovskite solar cells under vacuum and one atmosphere of nitrogen. Nature Energy, 2021, 6, 977-986.	19.8	103
38	Spray-Deposited Anisotropic Ferromagnetic Hybrid Polymer Films of PS- <i>b</i> -PMMA and Strontium Hexaferrite Magnetic Nanoplatelets. ACS Applied Materials & Interfaces, 2021, 13, 1592-1602.	4.0	8
39	Correlating Optical Reflectance with the Topology of Aluminum Nanocluster Layers Growing on Partially Conjugated Diblock Copolymer Templates. ACS Applied Materials & Interfaces, 2021, 13, 56663-56673.	4.0	9
40	Nucleation and Growth of Magnetron‣puttered Ag Nanoparticles as Witnessed by Timeâ€Resolved Small Angle Xâ€Ray Scattering. Particle and Particle Systems Characterization, 2020, 37, 1900436.	1.2	30
41	Following in Situ the Deposition of Gold Electrodes on Low Band Gap Polymer Films. ACS Applied Materials & Interfaces, 2020, 12, 1132-1141.	4.0	10
42	Internal nanoscale architecture and charge carrier dynamics of wide bandgap non-fullerene bulk heterojunction active layers in organic solar cells. Journal of Materials Chemistry A, 2020, 8, 23628-23636.	5.2	12
43	Novel highly substituted thiophene-based n-type organic semiconductor: structural study, optical anisotropy and molecular control. CrystEngComm, 2020, 22, 7095-7103.	1.3	2
44	Key Factor Study for Amphiphilic Block Copolymerâ€Templated Mesoporous SnO <sub>2</sub> Thin Film Synthesis: Influence of Solvent and Catalyst. Advanced Materials Interfaces, 2020, 7, 2001002.	1.9	9
45	Revealing structural evolution occurring from photo-initiated polymer network formation. Communications Chemistry, 2020, 3, .	2.0	11
46	Sodium Dodecylbenzene Sulfonate Interface Modification of Methylammonium Lead Iodide for Surface Passivation of Perovskite Solar Cells. ACS Applied Materials & Interfaces, 2020, 12, 52643-52651.	4.0	25
47	In Situ Studies of Solvent Additive Effects on the Morphology Development during Printing of Bulk Heterojunction Films for Organic Solar Cells. Small Methods, 2020, 4, 2000418.	4.6	20
48	Following <i>In Situ</i> the Evolution of Morphology and Optical Properties during Printing of Thin Films for Application in Non-Fullerene Acceptor Based Organic Solar Cells. ACS Applied Materials & Interfaces, 2020, 12, 40381-40392.	4.0	14
49	In situ Grazing-Incidence Small-Angle X-ray Scattering Observation of Gold Sputter Deposition on a PbS Quantum Dot Solid. ACS Applied Materials & Interfaces, 2020, 12, 46942-46952.	4.0	7
50	Lightâ€Induced and Oxygenâ€Mediated Degradation Processes in Photoactive Layers Based on PTB7â€Th. Advanced Photonics Research, 2020, 1, 2000047.	1.7	6
51	In Situ Study of Order Formation in Mesoporous Titania Thin Films Templated by a Diblock Copolymer during Slot-Die Printing. ACS Applied Materials & Interfaces, 2020, 12, 57627-57637.	4.0	10
52	In Situ Study of Sputtering Nanometer-Thick Gold Films onto 100-nm-Thick Spiro-OMeTAD Films: Implications for Perovskite Solar Cells. ACS Applied Nano Materials, 2020, 3, 5987-5994.	2.4	10
53	Balancing the pre-aggregation and crystallization kinetics enables high efficiency slot-die coated organic solar cells with reduced non-radiative recombination losses. Energy and Environmental Science, 2020, 13, 2467-2479.	15.6	69
54	Flow fields control nanostructural organization in semiflexible networks. Soft Matter, 2020, 16, 5439-5449.	1.2	14

#	Article	IF	CITATIONS
55	Tailoring of uniaxial magnetic anisotropy in Permalloy thin films using nanorippled Si substrates. Journal of Physics Condensed Matter, 2020, 32, 185804.	0.7	10
56	Colloidal PbS quantum dot stacking kinetics during deposition <i>via</i> printing. Nanoscale Horizons, 2020, 5, 880-885.	4.1	21
57	Core–Shell Nanoparticle Interface and Wetting Properties. Advanced Functional Materials, 2020, 30, 1907720.	7.8	22
58	Reorientation of π-conjugated molecules on few-layer MoS <sub>2</sub> films. Physical Chemistry Chemical Physics, 2020, 22, 3097-3104.	1.3	11
59	Mechanical and Morphological Properties of Lignin-Based Thermosets. ACS Applied Polymer Materials, 2020, 2, 668-676.	2.0	51
60	Correlating Nanostructure, Optical and Electronic Properties of Nanogranular Silver Layers during Polymer-Template-Assisted Sputter Deposition. ACS Applied Materials & Interfaces, 2019, 11, 29416-29426.	4.0	37
61	Effect of Solvent Additives on the Morphology and Device Performance of Printed Nonfullerene Acceptor Based Organic Solar Cells. ACS Applied Materials & Interfaces, 2019, 11, 42313-42321.	4.0	39
62	Structure–Function Correlations in Sputter Deposited Gold/Fluorocarbon Multilayers for Tuning Optical Response. Nanomaterials, 2019, 9, 1249.	1.9	12
63	Amphiphilic diblock copolymer-mediated structure control in nanoporous germanium-based thin films. Nanoscale, 2019, 11, 2048-2055.	2.8	10
64	Dual-Layer Nanofilms via Mussel-Inspiration and Silication for Non-Iridescent Structural Color Spectrum in Flexible Displays. ACS Applied Nano Materials, 2019, 2, 4556-4566.	2.4	22
65	Printed Thin Diblock Copolymer Films with Dense Magnetic Nanostructure. ACS Applied Materials & Interfaces, 2019, 11, 21935-21945.	4.0	8
66	Water-Induced Structural Rearrangements on the Nanoscale in Ultrathin Nanocellulose Films. Macromolecules, 2019, 52, 4721-4728.	2.2	58
67	Morphology Phase Diagram of Slotâ€Die Printed TiO <sub>2</sub> Films Based on Sol–Gel Synthesis. Advanced Materials Interfaces, 2019, 6, 1900558.	1.9	12
68	Functional Printing of Conductive Silver-Nanowire Photopolymer Composites. Scientific Reports, 2019, 9, 6465.	1.6	28
69	Sprayâ€Coating Magnetic Thin Hybrid Films of PSâ€∢i>bâ€PNIPAM and Magnetite Nanoparticles. Advanced Functional Materials, 2019, 29, 1808427.	7.8	17
70	Polymeric, Cost-Effective, Dopant-Free Hole Transport Materials for Efficient and Stable Perovskite Solar Cells. Journal of the American Chemical Society, 2019, 141, 19700-19707.	6.6	119
71	Composition–Morphology Correlation in PTB7-Th/PC <sub>71</sub> BM Blend Films for Organic Solar Cells. ACS Applied Materials & Interfaces, 2019, 11, 3125-3135.	4.0	30
72	Readily available titania nanostructuring routines based on mobility and polarity controlled phase separation of an amphiphilic diblock copolymer. Nanoscale, 2018, 10, 5325-5334.	2.8	16

#	Article	IF	CITATIONS
73	Three-Dimensional Orientation of Nanofibrils in Axially Symmetric Systems Using Small-Angle X-ray Scattering. Journal of Physical Chemistry C, 2018, 122, 6889-6899.	1.5	19
74	Comparison of UV Irradiation and Sintering on Mesoporous Spongelike ZnO Films Prepared from PS- <i>b</i> -P4VP Templated Sol–Gel Synthesis. ACS Applied Nano Materials, 2018, 1, 7139-7148.	2.4	6
75	Morphological properties of airbrush spray-deposited enzymatic cellulose thin films. Journal of Coatings Technology Research, 2018, 15, 759-769.	1.2	24
76	Magnetron-sputtered copper nanoparticles: lost in gas aggregation and found by <i>in situ</i> X-ray scattering. Nanoscale, 2018, 10, 18275-18281.	2.8	46
77	Tuning of the Morphology and Optoelectronic Properties of ZnO/P3HT/P3HT- <i>b</i> -PEO Hybrid Films via Spray Deposition Method. ACS Applied Materials & Interfaces, 2018, 10, 20569-20577.	4.0	9
78	Magnetic nanoparticle-containing soft–hard diblock copolymer films with high order. Nanoscale, 2018, 10, 11930-11941.	2.8	13
79	Effect of chain architecture on the swelling and thermal response of star-shaped thermo-responsive (poly(methoxy diethylene glycol acrylate)-block-polystyrene)3 block copolymer films. Soft Matter, 2018, 14, 6582-6594.	1.2	21
80	Impact of Catalytic Additive on Spray Deposited and Nanoporous Titania Thin Films Observed via <i>in Situ</i> X-ray Scattering: Implications for Enhanced Photovoltaics. ACS Applied Nano Materials, 2018, 1, 4227-4235.	2.4	5
81	Multiscale Control of Nanocellulose Assembly: Transferring Remarkable Nanoscale Fibril Mechanics to Macroscale Fibers. ACS Nano, 2018, 12, 6378-6388.	7.3	359
82	Critical Strains for Lamellae Deformation and Cavitation during Uniaxial Stretching of Annealed Isotactic Polypropylene. Macromolecules, 2018, 51, 6276-6290.	2.2	35
83	Role of Sputter Deposition Rate in Tailoring Nanogranular Gold Structures on Polymer Surfaces. ACS Applied Materials & Interfaces, 2017, 9, 5629-5637.	4.0	64
84	Flow-assisted assembly of nanostructured protein microfibers. Proceedings of the National Academy of Sciences of the United States of America, 2017, 114, 1232-1237.	3.3	77
85	Macroscale and Nanoscale Morphology Evolution during in Situ Spray Coating of Titania Films for Perovskite Solar Cells. ACS Applied Materials & Interfaces, 2017, 9, 43724-43732.	4.0	20
86	Investigating Polymer–Metal Interfaces by Grazing Incidence Small-Angle X-Ray Scattering from Gradients to Real-Time Studies. Nanomaterials, 2016, 6, 239.	1.9	31
87	Comparative study of the nanomorphology of spray and spin coated PTB7 polymer: Fullerene films. Polymer Engineering and Science, 2016, 56, 889-894.	1.5	22
88	Structural Changes of Gluten/Glycerol Plastics under Dry and Moist Conditions and during Tensile Tests. ACS Sustainable Chemistry and Engineering, 2016, 4, 3388-3397.	3.2	18
89	Manipulating the Assembly of Spray-Deposited Nanocolloids: <i>In Situ</i> Study and Monolayer Film Preparation. Langmuir, 2016, 32, 4251-4258.	1.6	30
90	A deep look into the spray coating process in real-time—the crucial role of x-rays. Journal of Physics Condensed Matter, 2016, 28, 403003.	0.7	26

#	Article	IF	CITATIONS
91	Spray Deposition of Titania Films with Incorporated Crystalline Nanoparticles for Allâ€Solidâ€State Dyeâ€Sensitized Solar Cells Using P3HT. Advanced Functional Materials, 2016, 26, 1498-1506.	7.8	53
92	Morphological Degradation in Low Bandgap Polymer Solar Cells – An In Operando Study. Advanced Energy Materials, 2016, 6, 1600712.	10.2	47
93	Real-Time Monitoring of Morphology and Optical Properties during Sputter Deposition for Tailoring Metal–Polymer Interfaces. ACS Applied Materials & Interfaces, 2015, 7, 13547-13556.	4.0	113
94	Distortion of Ultrathin Photocleavable Block Copolymer Films during Photocleavage and Nanopore Formation. Langmuir, 2015, 31, 8947-8952.	1.6	14
95	Improved Power Conversion Efficiency of P3HT:PCBM Organic Solar Cells by Strong Spin–Orbit Couplingâ€Induced Delayed Fluorescence. Advanced Energy Materials, 2015, 5, 1401770.	10.2	78
96	Following the Island Growth in Real Time: Ag Nanocluster Layer on Alq3 Thin Film. Journal of Physical Chemistry C, 2015, 119, 4406-4413.	1.5	16
97	Evaporation-Induced Block Copolymer Self-Assembly into Membranes Studied by <i>in Situ</i> Synchrotron SAXS. Macromolecules, 2015, 48, 1524-1530.	2.2	47
98	Patterned Diblock Co-Polymer Thin Films as Templates for Advanced Anisotropic Metal Nanostructures. ACS Applied Materials & Interfaces, 2015, 7, 12470-12477.	4.0	63
99	Arrangement of Maghemite Nanoparticles via Wet Chemical Self-Assembly in PS- <i>b</i> -PNIPAM Diblock Copolymer Films. ACS Applied Materials & Interfaces, 2015, 7, 13080-13091.	4.0	26
100	Templating growth of gold nanostructures with a CdSe quantum dot array. Nanoscale, 2015, 7, 9703-9714.	2.8	24
101	The Effect of Fluorination in Manipulating the Nanomorphology in PTB7:PC <sub>71</sub> BM Bulk Heterojunction Systems. Advanced Energy Materials, 2015, 5, 1401315.	10.2	68
102	Development of the Morphology during Functional Stack Build-up of P3HT:PCBM Bulk Heterojunction Solar Cells with Inverted Geometry. ACS Applied Materials & Interfaces, 2015, 7, 602-610.	4.0	25
103	Gyroidâ€Structured 3D ZnO Networks Made by Atomic Layer Deposition. Advanced Functional Materials, 2014, 24, 863-872.	7.8	68
104	Use of intermediate focus for grazing incidence small and wide angle x-ray scattering experiments at the beamline PO3 of PETRA III, DESY. Review of Scientific Instruments, 2014, 85, 043901.	0.6	40
105	Fast Diffusion-Limited Lyotropic Phase Transitions Studied in Situ Using Continuous Flow Microfluidics/Microfocus-SAXS. Langmuir, 2014, 30, 12494-12502.	1.6	42
106	Silver substrates for surface enhanced Raman scattering: Correlation between nanostructure and Raman scattering enhancement. Applied Physics Letters, 2014, 104, 243107.	1.5	103
107	Nano- and Microstructures of Magnetic Field-Guided Maghemite Nanoparticles in Diblock Copolymer Films. ACS Applied Materials & Interfaces, 2014, 6, 5244-5254.	4.0	30
108	Hydrodynamic alignment and assembly of nanofibrils resulting in strong cellulose filaments. Nature Communications, 2014, 5, 4018.	5.8	402

#	Article	IF	CITATIONS
109	Monitoring Structural Dynamics of Inâ€situ Sprayâ€Deposited Zinc Oxide Films for Application in Dyeâ€Sensitized Solar Cells. ChemSusChem, 2014, 7, 2140-2145.	3.6	28
110	A customizable software for fast reduction and analysis of large X-ray scattering data sets: applications of the new <i>DPDAK</i> package to small-angle X-ray scattering and grazing-incidence small-angle X-ray scattering. Journal of Applied Crystallography, 2014, 47, 1797-1803.	1.9	244
111	A quantitative approach to tune metal oxide network morphology based on grazing-incidence small-angle X-ray scattering investigations. Journal of Applied Crystallography, 2014, 47, 76-83.	1.9	7
112	In Situ Grazing Incidence Small-Angle X-ray Scattering Investigation of Polystyrene Nanoparticle Spray Deposition onto Silicon. Langmuir, 2013, 29, 11260-11266.	1.6	19
113	A Direct Evidence of Morphological Degradation on a Nanometer Scale in Polymer Solar Cells. Advanced Materials, 2013, 25, 6760-6764.	11.1	176
114	Lowâ€Temperature Solâ€Gel Synthesis of Nanostructured Polymer/Titania Hybrid Films based on Customâ€Made Poly(3â€Alkoxy Thiophene). ChemPhysChem, 2013, 14, 597-602.	1.0	11
115	From atoms to layers: in situ gold cluster growth kinetics during sputter deposition. Nanoscale, 2013, 5, 5053.	2.8	148
116	Cobalt Nanoparticles Growth on a Block Copolymer Thin Film: A Time-Resolved GISAXS Study. Langmuir, 2013, 29, 6331-6340.	1.6	52
117	Formation of Al Nanostructures on Alq3: An in Situ Grazing Incidence Small Angle X-ray Scattering Study during Radio Frequency Sputter Deposition. Journal of Physical Chemistry Letters, 2013, 4, 3170-3175.	2.1	36
118	In Situ X-ray Study of the Structural Evolution of Gold Nano-Domains by Spray Deposition on Thin Conductive P3HT Films. Langmuir, 2013, 29, 2490-2497.	1.6	46
119	Anisotropic particles align perpendicular to the flow direction in narrow microchannels. Proceedings of the National Academy of Sciences of the United States of America, 2013, 110, 6706-6711.	3.3	145
120	Combining mixed titania morphologies into a complex assembly thin film by iterative block-copolymer-based sol–gel templating. Nanotechnology, 2012, 23, 145602.	1.3	21
121	Pattern formation of colloidal suspensions by dipâ€coating: An in situ grazing incidence Xâ€ray scattering study. Physica Status Solidi - Rapid Research Letters, 2012, 6, 253-255.	1.2	20
122	Influence of Nanoparticle Surface Functionalization on the Thermal Stability of Colloidal Polystyrene Films. Langmuir, 2012, 28, 8230-8237.	1.6	24
123	PO3, the microfocus and nanofocus X-ray scattering (MiNaXS) beamline of the PETRA III storage ring: the microfocus endstation. Journal of Synchrotron Radiation, 2012, 19, 647-653.	1.0	253
124	Growth and Morphology of Sputtered Aluminum Thin Films on P3HT Surfaces. ACS Applied Materials & Interfaces, 2011, 3, 1055-1062.	4.0	45
125	Collapse transition in thin films of poly(methoxydiethylenglycol acrylate). Colloid and Polymer Science, 2011, 289, 569-581.	1.0	33
126	Solventâ€Induced Morphology in Polymerâ€Based Systems for Organic Photovoltaics. Advanced Functional Materials, 2011, 21, 3382-3391.	7.8	218

#	Article	IF	CITATIONS
127	<i>In situ</i> observation of cluster formation during nanoparticle solution casting on a colloidal film. Journal of Physics Condensed Matter, 2011, 23, 254208.	0.7	48
128	Global scattering functions: a tool for grazing incidence small angle X-ray scattering (GISAXS) data analysis of low correlated lateral structures. EPJ Applied Physics, 2010, 51, 10601.	0.3	14
129	Stripeâ€Like Pattern Formation in Airbrushâ€Spray Deposition of Colloidal Polymer Film. Advanced Engineering Materials, 2010, 12, 1235-1239.	1.6	14
130	Structural evolution of melt-drawn transparent high-density polyethylene during heating and annealing: Synchrotron small-angle X-ray scattering study. European Polymer Journal, 2010, 46, 1866-1877.	2.6	47
131	Two Lamellar to Fibrillar Transitions in the Tensile Deformation of High-Density Polyethylene. Macromolecules, 2010, 43, 4727-4732.	2.2	123
132	Swelling and switching kinetics of gold coated end-capped poly( <i>N</i> -isopropylacrylamide) thin films. Macromolecules, 2010, 43, 2444-2452.	2.2	51
133	Structural evolution of tensile deformed high-density polyethylene at elevated temperatures: Scanning synchrotron small- and wide-angle X-ray scattering studies. Polymer, 2009, 50, 4101-4111.	1.8	133
134	Polymer-Template-Assisted Growth of Gold Nanowires Using a Novel Flow-Stream Technique. Langmuir, 2009, 25, 11815-11821.	1.6	29
135	Colloidal silver nanoparticle gradient layer prepared by drying between two walls of different wettability. Journal of Physics Condensed Matter, 2009, 21, 264012.	0.7	8
136	Hierarchically Structured Titania Films Prepared by Polymer/Colloidal Templating. ACS Applied Materials & Interfaces, 2009, 1, 2862-2869.	4.0	80
137	In Situ GISAXS Study of Gold Film Growth on Conducting Polymer Films. ACS Applied Materials & Interfaces, 2009, 1, 353-360.	4.0	116
138	Array of Magnetic Nanoparticles via Particle Co-operated Self-Assembly in Block Copolymer Thin Film. Macromolecules, 2009, 42, 6202-6208.	2.2	38
139	Layered TiO2 :PVK nano-composite thin films for photovoltaic applications. European Physical Journal E, 2008, 26, 73-9.	0.7	24
140	Correlated Roughness in Polymer Films Containing Maghemite Nanoparticles. Macromolecules, 2008, 41, 2186-2194.	2.2	27
141	Characterization of Highly Porous Polymeric Materials with Pore Diameters Larger than 100 nm by Mercury Porosimetry and X-ray Scattering Methods. Langmuir, 2008, 24, 5877-5887.	1.6	25
142	In situ GISAXS Investigation of Gold Sputtering onto a Polymer Template. Langmuir, 2008, 24, 4265-4272.	1.6	52
143	In-Situ Observation of Drying Process of a Latex Droplet by Synchrotron Small-Angle X-ray Scattering. Macromolecules, 2008, 41, 5073-5076.	2.2	29
144	Thin Films of Poly( <i>N</i> -isopropylacrylamide) End-Capped with <i>n</i> -Butyltrithiocarbonate. Macromolecules, 2008, 41, 3209-3218.	2.2	63

#	Article	IF	CITATIONS
145	Maghemite Nanoparticles on Supported Diblock Copolymer Nanostructures. Macromolecules, 2007, 40, 5075-5083.	2.2	28
146	Structural changes in gradient colloidal thin gold films deposited from aqueous solution. Journal of Applied Crystallography, 2007, 40, s346-s349.	1.9	13
147	Flow in Confined Geometry Introduced by Dewetting of Ultrathin Polystyrene Films. Macromolecules, 2006, 39, 5087-5094.	2.2	16
148	Large-scale and local-scale structures in polymer-blend films: a grazing-incidence ultra-small-angle X-ray scattering and sub-microbeam grazing-incidence small-angle X-ray scattering investigation. Journal of Applied Crystallography, 2006, 40, s341-s345.	1.9	29
149	Combinatorial investigation of the isolated nanoparticle to coalescent layer transition in a gradient sputtered gold nanoparticle layer on top of polystyrene. Applied Physics Letters, 2006, 88, 021910.	1.5	46
150	Cell-wall recovery after irreversible deformation of wood. Nature Materials, 2003, 2, 810-813.	13.3	427
151	Self-assembled gradient nanoparticle-polymer multilayers investigated by an advanced characterization method: microbeam grazing incidence x-ray scattering. Applied Physics Letters, 2003, 82, 1935-1937.	1.5	86
152	Lowâ€Temperature and Waterâ€Based Biotemplating of Nanostructured Foamâ€Like Titania Films Using ßâ€Lactoglobulin. Advanced Functional Materials, 0, , 2113080.	7.8	5